Environmental Science & Technology

pubs.acs.org/est

Article

Sequential Oxidizing–Reducing Degradation of Organic Micropollutants in Simulated Riverbank Filtration

Yujia Zhai,[¶] Xun Wang,[¶] Xuhan Deng, Xiaoming Li, Bin Hu, Walter van der Meer, Mark C. M. van Loosdrecht, Gang Liu,* and Martin Pabst

Cite This: *Environ. Sci. Technol.* 2026, 60, 5804–5816

Read Online

ACCESS | Metrics & More | Article Recommendations | Supporting Information

ABSTRACT: Riverbank filtration is a nature-based water treatment strategy known for its effective removal of organic micropollutants. Yet, the mechanisms governing their biodegradation, especially the role of redox transitions in mediating biotransformation, remain insufficiently understood. Here, we integrate metagenomic profiling with chemical analytics in a 10 m simulated riverbank filtration system to demonstrate how sequential oxidizing–reducing degradation enhances organic micropollutant transformation. Oxygen stratification structured distinct microbial and enzymatic pathways: oxidizing zones (>+200 mV redox potential) facilitated cytochrome P450-mediated oxidation (oxidizing condition, OXD), while subsequent redox shifts to reducing conditions (←400 mV, sequential oxidizing–reducing (SOR) conditions) activated reductive transformations (e.g., via nitronate monooxygenase and aldehyde dehydrogenase) and conjugation pathways. These SOR conditions significantly enhanced the removal of recalcitrant compounds, including irbesartan (+25.3%), benzotriazole (13.4%), and gabapentin (+9.7%). Metagenomic analysis revealed redox-driven microbial specialization, with *Pseudomonadota* and *Nitrospirota* dominating in oxidizing zones and reducing microzones enriched in pathways associated with nitrotoluene and ethylbenzene degradation, providing genomic evidence for sequential organic micropollutant breakdown. These findings establish a mechanistic framework for harnessing oxidizing–reducing microbial partnerships to amplify organic micropollutant removal in nature-based water treatment systems, which can be used for riverbank filtration site selection and well field construction and optimization.

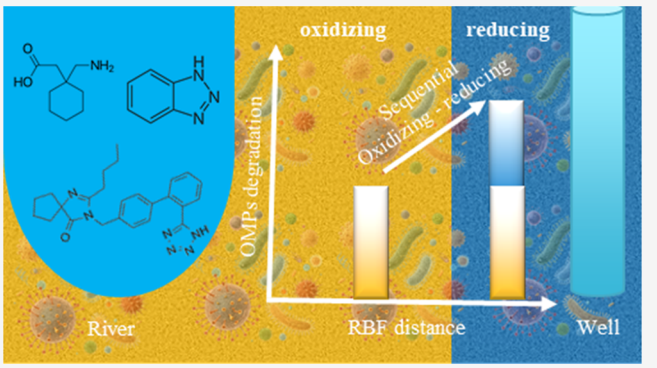

KEYWORDS: *metagenomics, organic micropollutant degradation, riverbank filtration, sequential oxidizing, reducing degradation*

1. INTRODUCTION

Riverbank filtration is a nature-based drinking water treatment technology in which river water infiltrates through adjacent alluvial sediments and aquifers before being abstracted from wells.[1] As the water moves through the subsurface, it undergoes physical filtration, adsorption, and microbially mediated biogeochemical transformations that collectively attenuate inorganic, organic, and microbial contaminants.[2] Riverbank filtration has been widely applied for more than a century, particularly along the River Rhine, and historically produced drinking water of high quality that little or no post-treatment was required in Germany during the early twentieth century.[3] As pollution increased, additional treatment steps became necessary such as activated carbon filtration and ozonation. Nevertheless, riverbank filtration has remained a robust and valuable pretreatment method, enabling more compact and cost-effective downstream treatment compared with direct river water abstraction.

Organic micropollutants, including pharmaceuticals, pesticides, and industrial chemicals, are increasingly detected in surface and groundwaters, raising significant environmental and public health concerns.[4,5] Their persistence results from chemical stability, slow biodegradation rates, and continuous anthropogenic inputs.[6,7] Advanced treatment technologies such as ozonation, activated carbon adsorption, and membrane filtration have been widely implemented to enhance removal.[8] However, these processes may exhibit variable efficiency, generate transformation products of uncertain toxicity, and impose substantial capital and operational costs.[9−11] Consequently, nature-based approaches, such as riverbank filtration, have gained attention for their potential to mitigate organic micropollutant contamination through natural attenuation mechanisms.[12,13]

Received: January 2, 2026
Revised: February 6, 2026
Accepted: February 9, 2026
Published: February 13, 2026

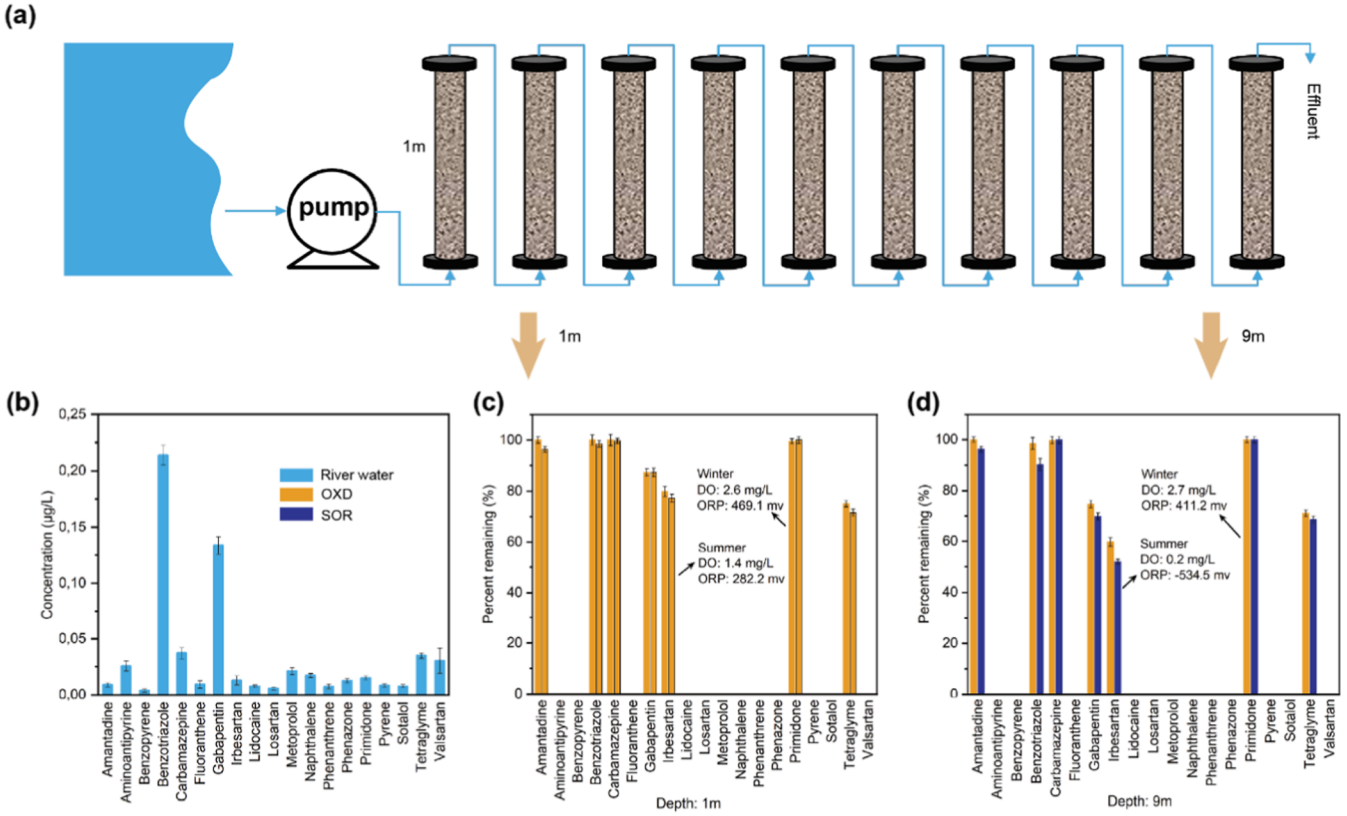

Figure 1. Experimental design and removal efficiencies of organic micropollutants under oxidizing (OXD) and sequential oxidizing−reducing (SOR) conditions. (A) Illustration of a 10-column system simulating riverbank filtration process; samples were taken from river after the 1st column and 9th column; (B) concentrations of the 19 organic micropollutants detected in river water; (C) removal of the 19 organic micropollutants by the 1st column (1 m) in summer and winter; and (D) removal of the 19 organic micropollutants by the 9th column (9 m) in summer and winter.

A defining characteristic of riverbank filtration is the development of dynamic redox gradients along the infiltration pathway, creating spatially distinct oxidizing and reducing zones that support diverse microbial metabolic processes relevant to organic micropollutant degradation.[3,14,15] Advances in metagenomics, bioinformatics, and high-resolution chemical analytics now allow more detailed characterization of these microbial functions, offering insight into metabolic pathways and enzymes involved in pollutant transformation.[16,17] Previous studies indicate that oxidative conditions promote degradation via monooxygenases and dioxygenases, whereas reductive environments facilitate transformations mediated by dehalogenases, reductases, and transferases.[18,19] However, redox conditions in field systems are often difficult to measure, inconsistently reported, and rarely paired with microbial community data. Laboratory studies integrate environmental variables, removal data, and metagenomic analyses, but they typically focus on early infiltration zones where the reducing conditions are not fully developed. As a result, the interactive influences of oxidizing, reducing, and sequential redox processes on micropollutant removal remain insufficiently understood.

In this study, we established a 10-column pilot-scale riverbank filtration system to reproduce the redox gradient characteristic of natural subsurface filtration environments. By integrating metagenomic sequencing with comprehensive chemical analyses, we investigated (i) how microbial communities and redox conditions evolve spatially and temporally during riverbank filtration; (ii) which functional genes and enzymes mediate organic micropollutant degradation; and (iii) the extent to which sequential oxidizing—reducing conditions enhance the removal of recalcitrant compounds such as benzotriazole, gabapentin, and irbesartan. The findings provide a mechanistic foundation for optimizing riverbank filtration design and operation to improve the sustainable removal of organic micropollutants from river water.

2. MATERIALS AND METHODS

2.1. Simulated Riverbank Filtration Setup

A pilot-scale experiment was conducted in Krimpen aan de Lek, South Holland, The Netherlands (51°53′44.2″N 4°38′29.9″E), utilizing two duplicate sets of 10 black PVC columns to simulate a riverbank filtration system (Figure 1a). Each column is 1 m in length and 200 mm in diameter, representing a 1 m horizontal section of riverbank filtration. The column was filled with technical sand characterized by a particle size range of 1.4−2 mm and a median diameter (d50) of 1.83 mm, added incrementally in 4−5 cm layers with manual tapping to prevent stratification. Each column was equipped with a redox potentiometer and a thermometer at the top for continuous monitoring of redox potential and temperature (Endress + Hauser, Germany), and valves were installed at both the top and bottom for soil and water sampling, respectively. To prevent air entrapment, the columns were interconnected via piping, maintaining a bottom-to-top flow direction. The entire system was operated in a darkened room to avoid algae growth and photolysis-induced organic micropollutant loss. The pilot was supplied with river water pumped directly from the Lek River, a tributary of the lower Rhine, at a hydraulic loading rate of 30 L/day, equivalent to a filtration rate of 1 m/day that is typical of

https://doi.org/10.1021/acs.est.5c18277
Environ. Sci. Technol. 2026, 60, 5804−5816

riverbank filtration fields, and yields residence times and redox conditions representative of full-scale systems.

2.2. Operation and Sampling

The first column (1 m) of the entire device represents the initial oxidizing condition (OXD) in riverbank filtration. To prevent possible influences to the 10th column from exposure to the outside air, we chose the ninth column (9 m) to represent the sequential oxidizing−reducing (SOR) conditions. The simulated riverbank filtration systems were operated under stable conditions for three years before starting sampling of this study from March to December 2023. River water (influent) and filtrated water (effluent) were sampled monthly to investigate composition and concentration of organic micropollutants present in the river and removed by a simulated riverbank filtration system. Water samples were filtered through polycarbonate filter paper (Merck Millipore, Germany) with a pore size of 0.2 μm. Besides, the sand samples were collected from the first column (top) and ninth column (bottom) in summer and winter for metagenomics analysis to investigate the microbial community related to organic micropollutant removal. All samples were taken and processed independently in duplicate (biological replicates). Water samples were kept on ice during transport and processed within 24 h. Sand samples were aliquoted into 2 mL cryotubes and stored at −80 °C until DNA isolation.

2.3. Organic Micropollutant Analysis

The organic micropollutants in water samples were extracted via solid phase extraction (SPE) using OASIS Prime HLB cartridges (Waters, Milford, MA, U.S.A.) and analyzed using a high-performance liquid chromatography-tandem mass spectrometry system (HPLC-MS/MS, API 6500 Q-TRAP) following the standard method.[20] Detailed description is given in Text S1 and Table S1.

2.4. DNA Extraction and Sequencing

DNA was extracted from the filters using the DNeasy Powersoil Kit (Qiagen, Germany) following the standard protocol; bead beating was set to 10 min, followed by a 4 min centrifugation at 4000*g*. The incubation time at 4 °C after the addition of inhibitor removal solution (IRS) was extended to 10 min. DNA was eluted in 60 mL of elution buffer. Subsequently, DNA concentration was measured on a Qubit2.0 fluorometer using a Qubit dsDNA HS Assay Kit (Invitrogen, OR, United States) following the manufacturer's instructions. One μL of DNA was added to 199 μL of working solution for measurement. Genomic DNA and all further DNA products were stored at −80 °C until processing. Sequencing libraries were generated using NEB Next Ultra DNA Library Prep Kit for Illumina (New England Biolabs, MA, USA) following the manufacturer's recommendations, and index codes were added. The library quality was assessed on the Qubit4.0 Fluorometer (Life Technologies, Grand Island, NY) and the Qsep 400 high-throughput nucleic acid protein analysis system (Houze Biological Technology Co, Hangzhou, China). Finally, the library was sequenced on an Illumina NovaSeq 6000 platform, and 150 bp paired-end reads were generated. The raw metagenome data for this study have been deposited in the European Nucleotide Archive (ENA) at EMBL-EBI under accession number PRJEB87202.

2.5. Metagenomics Analysis

The quality of the sequenced raw reads was assessed by FastQC (version 0.11.7) with default parameters[21] and visualized with MultiQC (version 1.0).[22] Low-quality paired-end reads were trimmed and filtered by Trimmomatic version 0.39 on the paired-end mode.[23] Taxonomic classification of raw reads was performed to profile the microbiome from each sample using the standard Kraken2 (version 2) database (uses all complete bacterial, archaeal, and viral genomes in the NCBI Refseq database) complemented with a curated wastewater database[24] with default parameters.[25] The taxonomic classification outcomes from Kraken2.0 were converted into abundance tables using the Pavian visualization tool[26] to explore metagenomics classification data sets. Figures were generated with the R package "phyloseq".[27] Clean reads were assembled into contigs using MetaSPAdes (version 3.13.0) with a k-mer spectrum of 21, 33, 71, 101, and 121.[28] Open reading frames (ORFs) were predicted using Prodigal,[29] followed by clustering with MMseqs2 under stringent parameters (sequence identity ≥0.9 and coverage ≥0.9).[30] Functional genes were annotated using eggNOG-mapper with recommended parameters (diamond, e-value = 1×10^{-5}).[31] And relative abundance (transcripts per million, TPM) of each sample was quantified using CoverM with stringent parameters to ensure accuracy: --min-read-percent-identity 90, --min-read-aligned-percent 50, --min-covered-fraction 0.5.[32]

2.6. Biotransformation Rule Extraction and Analysis

The EAWAG[33] and EnviPath[34] databases were utilized to predict the biotransformation pathways of organic micropollutants, covering all aerobic transformation probabilities. The associated EC numbers at the subsubclass level and corresponding genes for each biotransformation rule were extracted and summarized. For each OMP, candidate genes were retrieved from metagenomic data by using Python. Specifically, third-level EC numbers were compiled from EnviPath, and genes with matching IDs were extracted from the metagenomic data set into new Excel sheets via search and copy functions. A list of relevant biotransformation rules (bt rules), functional groups, and reaction types is provided in Table S2, along with the corresponding EC numbers for all 19 organic micropollutants. Additionally, heatmaps were generated using the ggplot2 package in R for visualization.[35]

2.7. Statistical Analysis of Functional Genes, Organic Micropollutant Degradation, and Microbial Consortium

The correlation analysis among functional genes, OMP degradation, and microbial consortium was performed as previously described.[17] In short, Pearson correlation coefficients (r) were computed using R (version 3.6.3) for the organic micropollutant degradation and gene abundances under the OXD and SOR conditions. Genes with a correlation coefficient of >0.6 were considered potential contributors to the OMP biotransformation. In the EC classification scheme, enzymatic reaction types are typically defined at the third level (subsubclass), while the fourth digit specifies substrate specificity. Thus, correlation analysis was conducted at the fourth-level EC numbers. Correlation coefficients and hierarchical clustering were performed using OmicStudio[36] to generate heatmaps based on the Euclidean distance and complete linkage. Furthermore, Mantel tests were conducted to assess the relationship between microbial abundance at the phylum level and gene accumulation under specific EC subsubclasses, with statistical significance set at $P < 0.05$ and Rho >0.5. Finally, SankeyMATIC was employed to visualize the connections between microbial consortia, gene accumulation, and OMP degradation.

3. RESULTS

3.1. ORP Variations and Organic Micropollutant Removal in Summer and Winter

As shown in Figure S1a, ORP varies across columns and seasons, which can be categorized as oxidizing (>+200 mV), transitional (−400 to +200 mV), or reducing (<−400 mV). The initial sections of the filter columns were predominantly under oxidizing condition, with ORP values exceeding +200 mV, referred to here as oxidizing treatment (OXD). As the filtration distance increased from the first to ninth column, oxygen consumption gradually led to reducing conditions, particularly in the final columns in summer, where ORP dropped below −400 mV. This summer ORP condition of the simulated riverbank filtration system is termed sequential oxidizing−reducing (SOR) conditions. ORP fluctuations closely correlated with offline measured dissolved oxygen and the seasonal water temperature variations (Figure S1b,c). In summer, peak temperatures (~25 °C) enhanced microbial growth and metabolic activity, whereas winter temperatures

https://doi.org/10.1021/acs.est.5c18277
Environ. Sci. Technol. 2026, 60, 5804−5816

(~10 °C) potentially slowed biodegradation, influencing organic micropollutant removal efficiency.

Figure 1 presents the concentrations and removal efficiencies of 19 detected organic micropollutants during simulated riverbank filtration by the first column (1 m, Figure 1c) and ninth column (9 m, Figure 1d) in the summer and winter. Across all seasons and depths, 12 of 19 organic micropollutants exhibited high removal efficiencies under OXD (~100%). Tetraglyme was partially removed by OXD (30−40%), while carbamazepine, primidone, and amantadine remained unaffected. Notably, irbesartan, gabapentin, and benzotriazole were partially removed, with significantly higher removal efficiencies observed in summer ($p < 0.01$). This enhancement, particularly under sequential oxidizing−reducing conditions in deeper sands (SOR), led to increased removal rates for irbesartan (+9.7%), gabapentin (+13.4%), and benzotriazole (+25.3%). These findings highlight the contribution of initial OXD pathways in organic micropollutant degradation, while the enhanced removal under SOR conditions demonstrates the critical role of redox-mediated microbial collaboration in degrading recalcitrant compounds such as irbesartan, gabapentin, and benzotriazole.

3.2. Enrichment of Genes, Genera, and Pathways

From the metagenome, a total of 14,175 unique KEGG ortholog IDs (KO IDs) were identified, each representing the functional characteristics of the detected genes. Out of all of the KO IDs, 7130 genes were associated with different ECs that best describe the enzymatic function of the genes. These enzymes belonged to oxidoreductases (EC 1, n = 1623), transferases (EC 2, n = 2428), hydrolases (EC 3, n = 1635), lyases (EC:4, n = 518), isomerases (EC5, n = 442), ligases (EC6, n = 273), and translocases (EC7, n = 211). Comparing OXD and SOR, the differential abundant genes, genera, and pathways are depicted in Figure 2. In general, there were 138 genes significantly higher in the level of the OXD and SOR, and the top 3 abundant genes were K03119 (taurine dioxygenase, involved in taurine and hypotaurine metabolism), K07795 (3-oxo-5-alpha-steroid 4-dehydrogenase, EC 1.3.99.5, involved in androgen and estrogen metabolism), and K07233 (4-hydroxyphenylpyruvate dioxygenase, EC 1.13.11.27, involved in tyrosine metabolism). There were 100 genes significantly higher in SOR than in OXD; the top 3 abundant genes were K01206 (beta-galactosidase, EC 3.2.1.23, involved in galactose metabolism), K10700 (phosphatidylserine decarboxylase, EC 4.1.1.65, involved in glycerophospholipid metabolism), and K01190 (alpha-galactosidase, EC 3.2.1.22, involved in galactose metabolism) (Figure 2a). Focusing on the SOR, the genes that can facilitate cometabolic degradation, particularly under anaerobic conditions following aerobic phases, were significantly enriched, such as K04561 (*norB*), K07550 (*nosZ*), K02679 (*narG*), K01668 (*nirK*), K06201 (*nirS*), K00880 (*ackA*), K03150 (*pta*), K00656 (*ldhA*), K00862 (*adhE*), and K01813 (*pfkA*).

For the microbes, *Planktophila* spp. and *Nitrospira* spp. were significantly higher abundances in OXD than in SOR (Figure 2b). The genera such as *Ignavibacterium* spp., *Limnobacter* spp., and *Melioribacter* spp. showed significantly higher abundance in the SOR than in the case of the OXD. These are anaerobic or facultative anaerobic bacteria and may collaborate with other microorganisms in anaerobic or low-oxygen environments to degrade or consummate organic pollutants. Additionally, KEGG pathways, including ko00511 and ko00603,

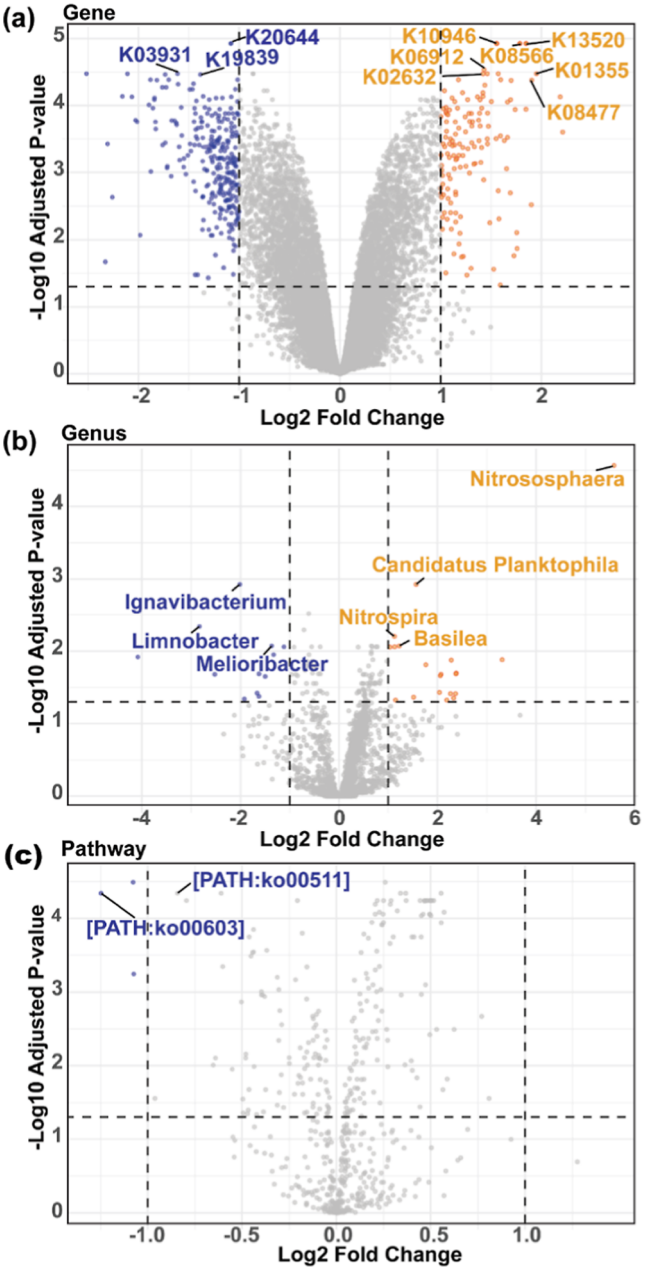

Figure 2. Enriched gene (a), genus (b), and pathways (c) by oxidizing and reducing conditions in simulated columns. In the volcano plots, dark blue dots represent enriched components in anaerobic conditions and brown dots represent enriched components in aerobic conditions.

were significantly upregulated in the SOR (Figure 2c). The enrichment of K19839 (cytochrome P450), K03931 (nitronate monooxygenase), and K20644 (aldehyde dehydrogenase) under SOR is consistent with the increased degradation of benzotriazole, gabapentin, and irbesartan. Metagenomic analysis revealed that the most abundant genes are functionally critical in organic micropollutant degradation pathways, including cytochrome P450 monooxygenases (CYP450s), aldehyde dehydrogenases (ALDHs), and nitronate monooxygenases. Specifically, CYP450s could catalyze initial hydroxylation of aromatic rings and aliphatic chains (e.g., in irbesartan and benzotriazole), ALDHs may oxidize aldehyde intermediates to prevent accumulation and promote mineralization, and

https://doi.org/10.1021/acs.est.5c18277
Environ. Sci. Technol. 2026, 60, 5804−5816

nitronate monooxygenases drive reductive transformation of nitroaromatic analogs under reducing conditions. The coenrichment of genes such as K07550 (nosZ, a thiolase involved in anaerobic aromatic degradation) and KO00603 (glyoxylate pathway) further indicates reductive processing and subsequent assimilation of intermediates into central carbon metabolism. The high abundance of these genes, particularly in SOR zones, supports their functional involvement in the observed enhanced degradation of the three organic micropollutants.

3.3. Functional Genes Related to Carbon and Nitrogen Cycles

The functional genes associated with carbon and nitrogen cycles were enriched differently in aerobic and anaerobic environments. In the carbon cycle (Figure 3a), the tricarboxylic acid (TCA) cycle displayed higher relative abundances of genes such as *frdA*, *smtA*, *mct*, and *aclB* in the aerobic zone compared to those in the anaerobic zone. This suggests a more active aerobic carbon metabolism in OXD.

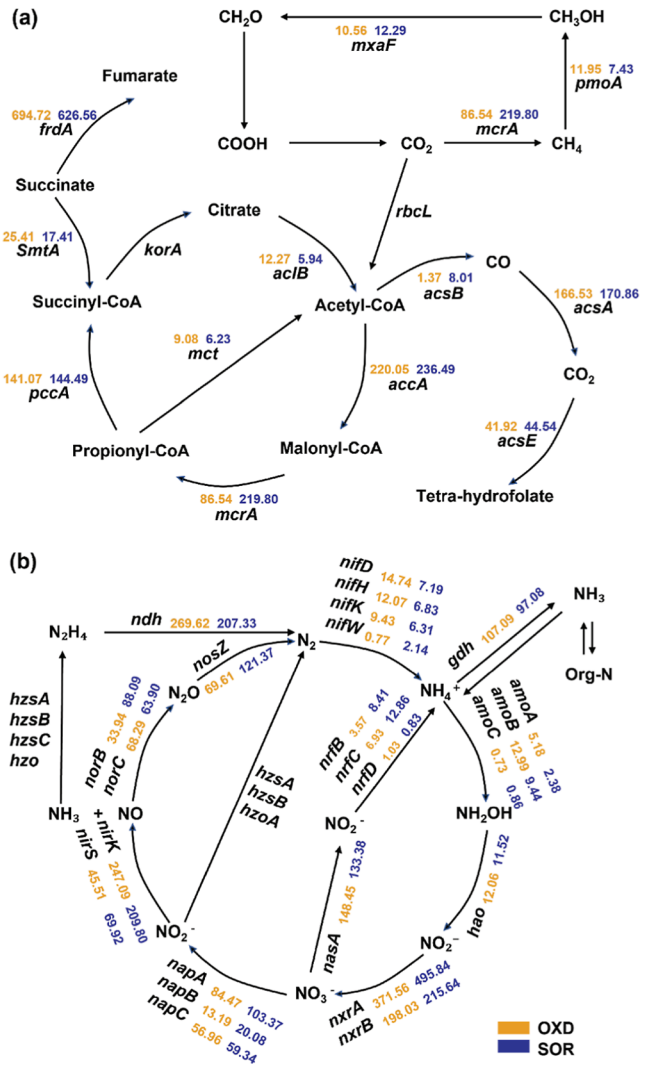

Figure 3. Relative abundances of functional genes involved in the (a) carbon and (b) nitrogen cycles. Brown represents oxidizing (OXD), and dark blue represents sequential oxidizing−reducing (SOR) zone. Values indicate relative abundances measured in transcripts per million.

Conversely, genes associated with anaerobic pathways showed higher relative abundances in SOR. Specifically, the *mcrA* gene, involved in the anaerobic methane cycle, and genes like *accA* and *acsB*, related to acetyl-CoA carboxylation and the anaerobic conversion of acetyl-CoA to CO, respectively, were more prevalent in SOR. This indicates a dominance of anaerobic carbon metabolism in SOR. These patterns reflect the differing oxygen availability and corresponding metabolic adaptations in the OXD and SOR environments.

For functional genes associated with the nitrogen cycle (Figure 3b), those genes involved in nitrification, such as *amoA*, *amoB*, *amoC*, *hao*, and *nxrA/B*, exhibited higher relative abundances in the OXD zone compared to those in the SOR zone (Figure 3b). Conversely, the SOR zone showed elevated levels of genes associated with anaerobic nitrogen processes, including denitrification (*narG*, *napA/B/C*, *nirK/S*, *norB/C*, and *nosZ*), nitrogen fixation (*nifH*), dissimilatory nitrate reduction to ammonium (DNRA; *nrfB/C/D*), and anaerobic ammonium oxidation (anammox; *hzsA*, *hzsB*, and *hzoA*). These patterns suggest a predominance of aerobic nitrogen processes in the OXD zone and sequential oxidizing−reducing processes in the SOR zone, which corresponded well to the above-mentioned carbon cycle.

3.4. Key Xenobiotics Metabolic Pathways and Enzymes of Organic Micropollutant Degradation

Similarly, key metabolic pathways involved in xenobiotic degradation were different between the aerobic and anaerobic zones (Figure 4). Notably, pathways such as drug and xenobiotic metabolism, halogenated compound degradation, and polycyclic aromatic hydrocarbon degradation were more prevalent in the OXD zone compared to those in the SOR zone. This observation aligns with the high performance of organic micropollutants removal in the OXD zone, where 12 out of 19 organic micropollutants were completely removed. Conversely, the SOR zone exhibited enrichment in the nitrotoluene degradation (ko00633) and ethylbenzene degradation (ko00642) pathways.

To better characterize organic micropollutant degradation, the presence or absence of key degrading enzymes was analyzed by mapping them onto the known metabolic pathways of benzopyrene, lidocaine, naphthalene, and carbamazepine (Figure 5). Key enzymes such as CYP3A4, CYP1A1, glutathione S-transferase (GST), and epoxide hydrolase 1 (EPHX1) were widely detected in both the OXD and SOR zones, correlating with the high removal efficiencies observed for benzopyrene, lidocaine, and naphthalene. For instance, benzopyrene can be metabolized into intermediates like 9-hydroxybenzopyrene-4,5-oxide, 4,5-dihydro-4-hydroxy-5-S-glutathionyl-benzopyrene, or 7,8-dihydro-7-hydroxy-8-S-glutathionyl-benzopyrene, while lidocaine can be metabolized into monoethyl glycinexylidide or 3-hydroxylidocaine. However, the absence of key enzymes such as CYP2B6 and CYP2C8, essential for carbamazepine degradation, resulted in its persistence across both oxidizing and sequential oxidizing−reducing conditions.

3.5. Identifying Organic Micropollutant-Specific Degradation Enzyme Candidates

Among the 19 organic micropollutants studied, 12 were completely removed (associate gene given in Figure S2), primarily through aerobic processes, with no significant differences in removal efficiencies between the oxidizing (OXD) and sequential oxidizing−reducing (SOR) conditions

https://doi.org/10.1021/acs.est.5c18277
Environ. Sci. Technol. 2026, 60, 5804−5816

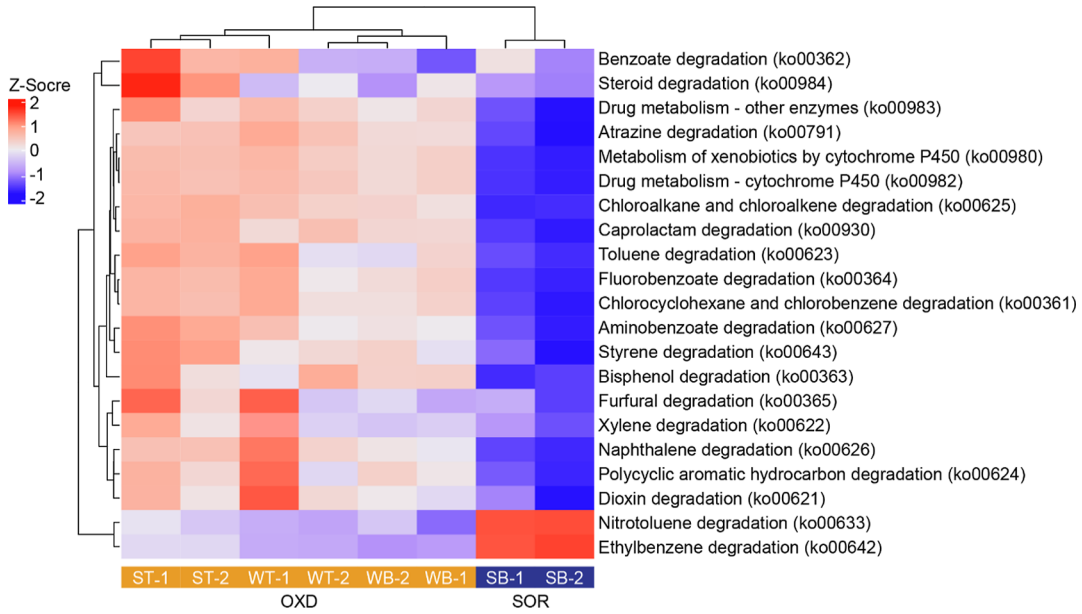

Figure 4. Enrichment of key xenobiotics metabolic pathways in OXD and SOR zones. Brown color bar represents the OXD zone, and dark blue color bar represents the SOR zone. Heat colors indicate relative abundances measured in transcripts per million (TPM) normalized as Z-score. Most of the pathways were enriched in OXD zones, while two pathways clearly enriched only in SOR zones (ko00633, ko00642).

(both 100%). However, three organic micropollutants (benzotriazole, irbesartan, and gabapentin) exhibited statistically significant differences in removal efficiencies between the OXD and SOR. This variation enabled a correlation analysis to identify potential degrader enzymes associated with their degradation, as detailed in Figure 6.

For benzotriazole, the top 50 genes with strong correlations ($r > 0.6$) are summarized in Figure 6a, including 59 oxidoreductases (EC 1) and 1 lyase (EC 4). Among them, oxidoreductases EC 1.3.1.- (e.g., K10780, K10797), which catalyze the oxidation of CH−CH groups using NAD (+) or NADP (+) as electron acceptors, were notably abundant in anaerobic environments (SB-1, SB-2). These enzymes likely play a crucial role in the initial oxidative transformation of benzotriazole. Additionally, lyases EC 4.99.1.- (K02304), which facilitate C−C and C−N bond cleavages via non-hydrolytic mechanisms, were also detected. For irbesartan, 58 oxidoreductases (EC 1) and 2 hydrolases (EC 3) exhibited strong correlations with degradation (Figure 6b). Notably, EC 1.13.12.- (K00486, K00459) and EC 1.14.13.- (K02609), which function as monooxygenases or mixed-function oxidases by incorporating molecular oxygen, were enriched in sequential oxidizing−reducing (SOR) zones. These enzymes likely target functional groups, such as CH, CH_2, oxo, and CH−NH in irbesartan, facilitating its breakdown. For gabapentin, degradation involved a broader enzymatic repertoire, including 10 oxidoreductases (EC 1), 8 transferases (EC 2), and 1 hydrolase (EC 3) (Figure 6c). Oxygenases EC 1.13.12.- (K00459) and dehydrogenases EC 1.4.1.- (e.g., K00259, K00261, and K00262) may be key players in targeting CH−NH_2 and CH−NH groups. Additionally, transaminases EC 2.6.1.- (e.g., K07250, K00831) and hydrolases EC 3.5.4.- (K01491), which act on carbon−nitrogen bonds excluding peptide bonds, were significantly enriched in SOR, suggesting their involvement in gabapentin breakdown under anaerobic conditions.

3.6. Linking Organic Micropollutant Degradation with Biotransformation Rules, Key Enzymes, and Microbes

Analysis of the interrelationships among irbesartan, benzotriazole, and gabapentin highlights their associated enzyme commission (EC) subsubclasses through specific biotransformation rules (bt rules), along with the microbial phyla linked to each EC subsubclass (Figure 7). Benzotriazole degradation is primarily associated with biotransformation rule bt0005, which involves amination reactions. The degradation pathway of gabapentin is linked to biotransformation rule bt0063, pertaining to the hydroxylation of aromatic rings. Irbesartan degradation encompasses multiple biotransformation rules, including bt0242 (glucuronidation), bt0243 (heparan sulfate degradation), and bt0334 (urease activity).

The enzymatic degradation of these organic micropollutants involves a diverse array of enzyme classes, including oxidoreductases (EC 1); these enzymes catalyze oxidation−reduction reactions, facilitating the transfer of electrons; transferases (EC 2), enzymes that catalyze the transfer of functional groups between molecules; and hydrolases (EC 3), enzymes that catalyze the hydrolysis of various bonds. The subsubclass includes EC 1.3, acting on the CH−CH group of donors; EC 1.13, incorporating molecular oxygen into substrates; EC 1.4, acting on the CH−NH_2 group of donors; EC 1.14, incorporating or reducing molecular oxygen with paired donors; EC 1.5, acting on the CH−NH group of donors; EC 1.17, acting on CH or CH_2 groups; EC 2.6, transferring nitrogenous groups; and EC 3.3, acting on ether bonds.

The microbial communities facilitating the degradation of these organic micropollutants predominantly consist of the following phyla: *Pseudomonadota*, *Thermodesulfobacteriota*, *Planctomycetota*, *Nitrospirota*, and *Bacillota*. These microbial communities and their associated enzymatic activities collectively play a crucial role in the environmental degradation and transformation of these organic micropollutants, contributing to the mitigation of pollution. For example, irbesartan

https://doi.org/10.1021/acs.est.5c18277
Environ. Sci. Technol. 2026, 60, 5804−5816

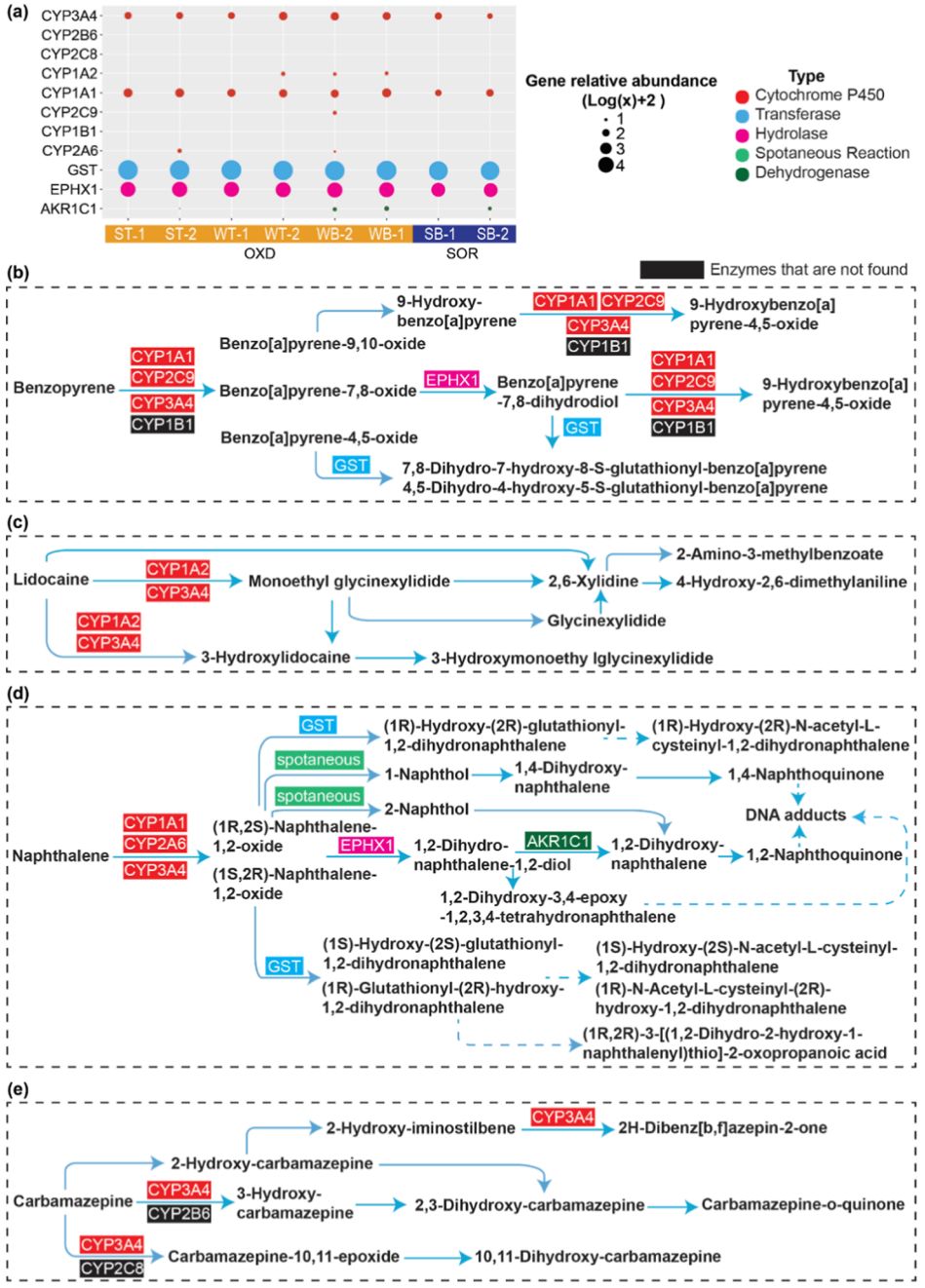

Figure 5. Enrichment of key enzymes in oxidizing and reducing zones for organic micropollutant degradation. Panels: (a) bubble plot illustrates the presence and relative abundance of key enzymes involved in OMP degradation within OXD and SOR zones. (b) The known degradation pathway for benzopyrene with key enzymes marked. (c) The known degradation pathway for lidocaine with key enzymes marked. (d) The known naphthalene degradation pathway with key enzymes marked. (e) The known carbamazepine degradation pathway with key enzymes marked. Notably, the anaerobic zone exhibited a significant enrichment of specific enzymes associated with the degradation of these compounds.

might be degraded through bt0243 via EC:1.14.14 by *Planctomycetota* and *Nitrospirota*.

4. DISCUSSION

Our study investigated the degradation of organic micropollutants during simulated riverbank filtration under varying redox conditions and seasonal influences. Metagenomic analysis revealed the stratification of functional genes, key enzymes, and biodegradation pathways along the riverbank filtration depth (1−9 m). While the oxidizing treatment (OXD) efficiently removed 12 out of 19 organic micropollutants (100%), it is noteworthy that sequential oxidizing−reducing (SOR) treatment played a critical role in metabolizing certain recalcitrant compounds (3 out of 19 organic micropollutants).

4.1. Redox and Microbiome Zonation along Filtration Distance of Riverbank

Our study underscores the significant influence of temperature on redox zonation within riverbank filtration systems. The observed oxidation−reduction potential (ORP) profiles (Figure S1) indicate that the initial sections of the filtration columns operated under oxidizing conditions (OXD; ORP > +

https://doi.org/10.1021/acs.est.5c18277
Environ. Sci. Technol. 2026, 60, 5804−5816

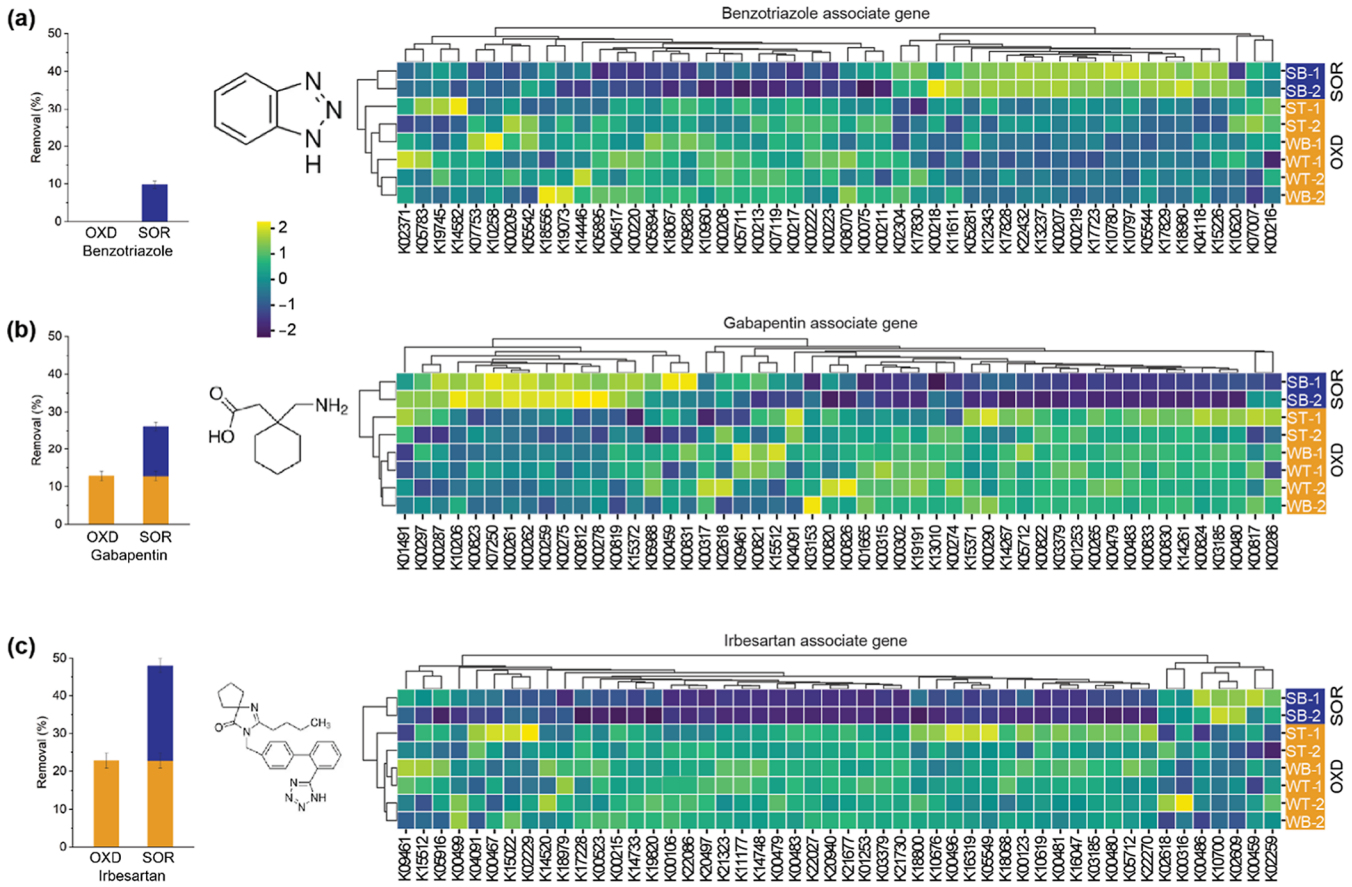

Figure 6. Degradation of benzotriazole, irbesartan, and gabapentin and associated gene candidates (top 50). Panels: (a) illustrates the removal efficiency of benzotriazole, its chemical structure, and the associated gene candidates. (b) Illustrates the removal efficiency of irbesartan, its chemical structure, and the associated gene candidates. (c) Illustrates the removal efficiency of gabapentin, its chemical structure, and the associated gene candidates. Notably, the sequential oxidizing–reducing (SOR) conditions exhibited significantly increased removal efficiencies for these compounds, corroborated by the elevated abundance of corresponding gene candidates.

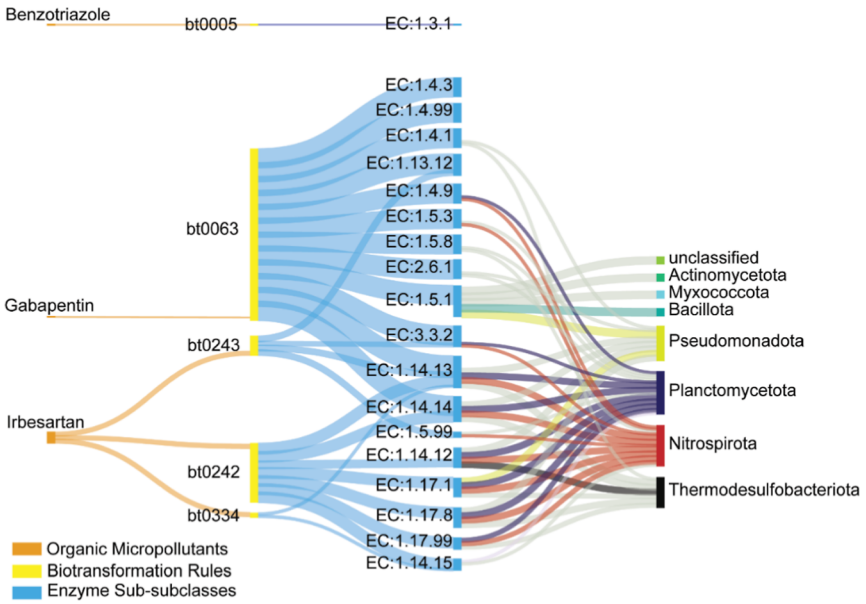

Figure 7. Network analysis of cometabolic degradation pathways of organic micropollutants. This network illustrates the interconnections among OMP structures, biotransformation rules, enzyme subsubclasses, and bacterial phyla. Highlighted are the organic micropollutants—benzotriazole, irbesartan, and gabapentin—that exhibited enhanced degradation under anaerobic conditions. The network provides insights into the microbial enzymes and metabolic pathways involved in the cometabolic degradation of these pollutants.

https://doi.org/10.1021/acs.est.5c18277
Environ. Sci. Technol. 2026, 60, 5804−5816

200 mV), while deeper sections, particularly during summer months, transitioned to reducing conditions (SOR; ORP < −400 mV in August). Seasonal temperature variations, approximately 25 °C in summer versus 10 °C in winter, appear to enhance oxygen consumption and microbial activity during warmer periods. This observation aligns with previous research highlighting the impact of temperature on redox zonation in both fields and simulated riverbank filtration systems.[12,37,38] Notably, such oxygen gradients may not be replicated in short column simulations focusing solely on the first meter of riverbank filtration systems. Considering typical ORP thresholds for aerobic (>200 mV), anoxic (−200 mV to 200 mV), and anaerobic (<−200 mV) conditions,[12,39,40] our study found that anoxic conditions were achieved at the second column in August (>25 °C), third column in July and September (∼23 °C), and seventh column in June and October (15−20 °C). Anaerobic conditions were only observed at the 10th column in July and fourth column in August. These findings highlight the importance of conducting studies with long enough water travel distance, especially when considering the critical roles of anaerobic or anoxic zones in water purification.

However, changes in the measured oxidation−reduction potential induced by temperature or filtration depth do not necessarily correspond to changes in pollutant removal, unless the underlying redox regime or the functional microbial community is altered. Metagenomic analysis revealed microbiome zonation aligned with redox gradients, with *Candidatus Planktophila* spp. and *Nitrospira* spp. predominating in the oxidizing column (1st column), consistent with their known roles in nitrogen assimilation and nitrification/complete ammonia oxidation in oxic freshwater systems.[41−43] In contrast, the SOR column (9th column in summer) was enriched in *Ignavibacterium*, *Limnobacter*, and *Melioribacter* spp., facultatively anaerobic organotrophs and thiosulfate oxidizers capable of sulfur- and iron-linked respiration and, in the case of *Limnobacter*, coupling reduced sulfur oxidation to nitrate reduction or denitrification.[44−47] These metabolic capacities are consistent with the observed redox stratification and support a mechanism in which oxidizing and reducing communities jointly contribute to nitrogen and organic micropollutant transformation along the filtration path.

The differentiation was also reflected in the enrichment of distinct metabolic pathways under the conditions of the OXD and SOR conditions. Consistent with higher organic micropollutant degradation efficiency in oxidizing conditions, pathways involving cytochrome P450 (CYP450) and oxygenase enzymes were significantly enriched, including drug and xenobiotic metabolism, halogenated compound degradation, and polycyclic aromatic hydrocarbon breakdown. In contrast, SOR exhibited enrichment in pathways associated with reduction reactions, such as the degradation of nitrotoluenes, ethylbenzene, and steroids. Regarding carbon and nitrogen cycling, aerobic treatment predominantly featured aerobic metabolic pathways, such as the TCA cycle and nitrification, while SOR was characterized by reducing processes including methane metabolism, denitrification, and anammox. These findings align with previous studies on the typical enzymes and metabolic pathways under different oxygen conditions,[48,49] highlighting the crucial role of oxygen in shaping microbiome composition, function, and evolution.[50] Meanwhile, it also indicates that the OXD treatment and SOR may perform differently on organic pollutant degradation.

4.2. Organic Micropollutant Degradation in Oxidizing and Reducing Conditions

Redox conditions play a crucial role in the degradation of organic micropollutants in riverbank filtration systems.[51] In this study, we observed that 12 out of the 19 detected organic micropollutants, those that have a structure that aerobic microbe can oxidize (aromatic rings, amines, amides) and tend to sorb to biomass, were efficiently removed in the first column, primarily through aerobic degradation. This finding aligns with previous research highlighting the significant role of the first meter of the riverbank in OMP removal, as demonstrated by both in situ field studies[52,53] and laboratory simulations.[13] In a laboratory-based 1 m column study, Zhao et al. (2022) reported that 82 out of 128 organic micropollutants were effectively removed (>70%) through biodegradation, including Lidocaine and Sotalol—compounds that were also efficiently removed in our study.[13] Furthermore, the degradation of metoprolol and naphthalene has been widely reported in various studies,[54−57] while primidone and carbamazepine have been consistently observed as persistent contaminants.[52,58,59] Carbamazepine degradation is known to be most effective under strongly reducing conditions (e.g., sulfate-reducing or methanogenic). Its persistence in our study is likely due to the fact that the columns did not maintain consistently strict anaerobic conditions.

Notably, we quantified the enhanced removal of benzotriazole, gabapentin, and irbesartan along the depth in riverbank filtration following SOR. Compared to that with OXD alone, removal efficiencies increased from 0 to 9.8% for benzotriazole, 12.8% to 26.2% for gabapentin, and 22.7% to 48.0% for irbesartan. This pattern of initial oxidation followed by reductive transformation aligns with prior studies of aromatic hydrocarbons, where monooxygenase-driven hydroxylation produces reactive intermediates that subsequently undergo anaerobic processing. In our system, the enrichment of cytochrome P450s (K19839) and nitronate monooxygenase (K03931) supports early oxidative activation of benzotriazole, gabapentin, and irbesartan, while the presence of anaerobic aromatic degradation genes, such as K07550 and the glyoxylate pathway (KO00603), indicates subsequent reductive metabolism of the resulting intermediates. Although only a few compounds showed enhanced biodegradation, the results indicate that sequential oxidizing and reducing conditions can meaningfully improve the organic micropollutant removal. The site water contained just 19 detectable compounds, so the three affected pollutants likely represent a significant share of the biodegradable fraction. Our pilot system achieved reducing conditions only during the summer and over a short travel distance. It represents a controlled proxy for natural RBF, whereas full-scale riverbank filtration systems maintain anaerobic zones for much longer distances, suggesting that the improvements observed here are conservative.[60−62] These findings highlight the potential to enhance riverbank filtration performance by increasing travel time or distance through well-field design and pumping strategies and by integrating redox monitoring for real-time operational control.

Numerous studies have documented the degradation or persistence of benzotriazole, gabapentin, and irbesartan in riverbank filtration and managed aquifer recharge (MAR) systems.[52,63−69] Benzotriazole, in particular, is widely recognized as effectively removed in riverbank filtration, with reported removal rates of 75%−90% at two sites in Berlin.[67] A comparative study using aquifer sediment from Bolivar, South

https://doi.org/10.1021/acs.est.5c18277
Environ. Sci. Technol. 2026, 60, 5804−5816

Australia, further demonstrated that aerobic treatment achieved higher benzotriazole degradation than anaerobic treatment (72% vs 48%).[70] For irbesartan and gabapentin, Nikolenko et al. (2024) reported their effective removal at aquifer sites in Barcelona, Spain,[69] while Schaper et al. (2019) observed similar removal patterns in the hyporheic zone of the Erpe River in Berlin, Germany.[64] However, conflicting results have been reported—Höhne et al. (2022) and Reith et al. (2023) found gabapentin to be effectively degraded, whereas irbesartan persisted.[65,66] These discrepancies in degradation performance, as well as the contradictory findings regarding specific compounds, may be attributed to variations in the redox conditions and microbial metabolism across field sites and sampling times. Since redox conditions are often challenging to measure and inconsistently reported in field studies, and microbiome data are frequently missing, these findings emphasize the importance of integrating metagenomic analysis with chemical removal data to better understand OMP degradation mechanisms in riverbank filtration systems.

4.3. Metagenomic Insights on Benzotriazole, Gabapentin, and Irbesartan Degradation

This 10-column study allowed us to simulate the redox gradient observed in field riverbank filtration systems and to explore the corresponding influences on organic micropollutant degradation and microbial metabolism. As mentioned above, we observed higher removal efficiencies of benzotriazole, gabapentin, and irbesartan under sequential oxidizing and reducing (SOR) conditions compared with oxidizing conditions alone, indicating that SOR metabolism enhanced their removal. By integrating the chemical structures of these organic micropollutants with metagenomic data, we proposed potential degradation pathways for benzotriazole, gabapentin, and irbesartan (Figures 6 and 7), which remain scarcely described in the literature due to the limited number of metagenomic studies on their transformation. It is proposed that their metabolism is closely associated with specific microbial groups, including *Bacillota*, *Pseudomonadota*, *Planctomycetota*, *Nitrospirota*, and *Thermodesulfobacteriota*, via bt0005 (benzotriazole), bt0063 (gabapentin), and bt0242, bt0243, and bt0334 (irbesartan).

Benzotriazole's aerobic degradation has been documented, notably by *Bacillus* sp. DH-12 in activated sludge, involving methylation and carboxylation steps.[71] Additionally, studies have shown that the presence of ammonia enhances benzotriazole biodegradation in both activated sludge and drinking water rapid sand filters, likely due to cometabolism with nitrification processes.[72,73] From a structure−function perspective, the triazole ring in benzotriazole is relatively resistant to direct oxidative cleavage, but adjacent carbon−nitrogen positions and ring substituents provide plausible sites for monooxygenase-mediated hydroxylation or methylation, which can destabilize the heterocycle and facilitate subsequent transformation. However, information about benzotriazole degradation via combined aerobic and anaerobic metabolism is scarce. One study proposed a potential association between bt0005 and the cometabolic degradation of organic micropollutants in wastewater.[17] Our findings suggest a previously unexplored synergistic enhancement of benzotriazole degradation through aerobic−anaerobic processes, although our current data do not yet resolve the specific enzymes and reaction steps involved.

For gabapentin, our data (Figure 7) suggest that a possible pathway may involve initial hydroxylation of the cyclohexane ring by monooxygenases (EC 1.14.13.-) from aerobic microbes such as *Pseudomonadota*, forming hydroxylated gabapentin intermediates. The saturated cyclohexane ring provides accessible sites for such hydroxylation, which can increase the ring strain and reactivity. Subsequently, Baeyer−Villiger monooxygenases (EC 1.14.13.-) may catalyze lactonization, leading to ring cleavage and the formation of open-chain carbonylated compounds. Under anaerobic conditions, the primary amine group in gabapentin is a likely target for deaminases (EC 1.4.99.-), which may convert it to ammonium (NH_4^+) that can be further transformed into nitrogen gas (N_2). However, the current literature does not provide direct evidence for this specific sequence of hydroxylation, lactonization, and deamination. A study by Henning et al. (2010) investigated the biotransformation of gabapentin under different redox conditions in water−sediment systems and observed rapid elimination under aerobic conditions, while no decrease was observed under strictly anaerobic conditions.[74] This differs from our results, possibly due to differences in the anaerobic environment compared to the aerobic−anaerobic dual treatment employed in our study. Moreover, Henning et al. identified eight biological transformation products, with the most relevant being gabapentin-lactam, formed via intramolecular amidation (up to 18% of the initial gabapentin concentration), suggesting an alternative pathway involving intramolecular reactions rather than the proposed hydroxylation and lactonization steps. Another study using aerobic starved activated sludge linked gabapentin degradation to genera such as *Kinneretia* spp., *Cytophagaceae* spp., and *Saprospiraceae* spp.[75] but did not assess anaerobic performance. In addition, research using model microbial communities combined with metagenomics indicated an association between gabapentin degradation and methyltransferase activity,[76] suggesting the existence of further unexplored functions and pathways involved in gabapentin biotransformation.

In summary, although the proposed pathway for gabapentin degradation is theoretically plausible, direct experimental evidence supporting this sequence of reactions is currently lacking. The degradation pathways of irbesartan remain largely unexplored; structural considerations similarly point to potential enzymatic targets. The biphenyl moiety is a typical substrate for aromatic mono- and dioxygenases, which can introduce hydroxyl groups and initiate ring activation. Furthermore, the heteroatom-containing imidazolinone and tetrazole rings provide sites that may undergo nucleophilic attack, oxidative modification, or reductive ring opening once the molecule has been partially activated. Although direct experimental evidence for these transformations remains limited, the combination of these functional group properties and the presence of relevant gene families (bt0242, bt0243, and bt0334) in the metagenomes supports the plausibility of the proposed pathways while underlining the need for targeted metabolite and enzyme-level studies.

More broadly, the mechanistic basis of enhanced organic micropollutant removal under sequential oxidizing−reducing conditions remains insufficiently understood. While our findings reveal clear improvements in the removal of several organic micropollutants and point to potential transformation pathways, further in-depth investigations are needed to identify the specific microbial taxa, enzymes, and metabolic routes

https://doi.org/10.1021/acs.est.5c18277
Environ. Sci. Technol. 2026, 60, 5804−5816

responsible for these processes. Advancing this understanding would support the development of sustainable management strategies for addressing the global challenge posed by organic micropollutants, including through riverbank filtration or other managed aquifer recharge approaches.

A limitation of this study is that biodegradation intermediates of benzotriazole, gabapentin, and irbesartan were not measured. While our metagenomic and redox-dependent removal patterns provide evidence for plausible transformation pathways, definitive confirmation of these routes requires approaches capable of capturing metabolic processes and characterizing intermediate metabolites. Future work integrating RNA-based metatranscriptomics, targeted or nontargeted high-resolution mass spectrometry, isotope-assisted metabolite tracing, and time-resolved sampling would be valuable for validating the proposed mechanisms and identifying active degradation steps along the filtration pathway. Future research should also focus on assessing the role of redox-active solids, which may contribute significantly to the degradation of organic micropollutant degradation.

■ ASSOCIATED CONTENT

Data Availability Statement

Sequence data associated with this project have been deposited in the NCBI Short Read Archive database (Accession Number: PRJEB87202).

Supporting Information

The Supporting Information is available free of charge at https://pubs.acs.org/doi/10.1021/acs.est.5c18277.

Organic micropollutant analysis by LCMS (Text S1); time series data of simulation system (Figure S1); gene candidates (top 50) of the other 16 organic micropollutants (Figure S2); water quality parameters over the course of the study (Table S1); INTERNAL standards used in this study (Table S2); and organic micropollutants with predicted biotransformation rules and EC subclasses (Table S3) (PDF)

■ AUTHOR INFORMATION

Corresponding Author

Gang Liu − *Key Lab of Aquatic Chemistry, State Key Lab of Regional Environment and Sustainability, Research Centre for Eco-Environmental Sciences, Chinese Academy of Sciences, Beijing 100085, China; University of Chinese Academy of Sciences, Beijing 101408, China;* orcid.org/0000-0002-4008-9017; Email: gliu@rcees.ac.cn, g.liu-1@tudelft.nl

Authors

Yujia Zhai − *State Key Laboratory of Wetland Conservation and Restoration, School of Environment, Beijing Normal University, Beijing 100875, China; Department of Biotechnology, Delft University of Technology, Delft 2629 HZ, The Netherlands*

Xun Wang − *Department of Biotechnology, Delft University of Technology, Delft 2629 HZ, The Netherlands; Sanitary Engineering, Department of Water Management, Delft University of Technology, Delft 2628 CN, The Netherlands; Key Lab of Aquatic Chemistry, State Key Lab of Regional Environment and Sustainability, Research Centre for Eco-Environmental Sciences, Chinese Academy of Sciences, Beijing 100085, China*

Xuhan Deng − *Sanitary Engineering, Department of Water Management, Delft University of Technology, Delft 2628 CN, The Netherlands; Key Lab of Aquatic Chemistry, State Key Lab of Regional Environment and Sustainability, Research Centre for Eco-Environmental Sciences, Chinese Academy of Sciences, Beijing 100085, China*

Xiaoming Li − *Key Lab of Aquatic Chemistry, State Key Lab of Regional Environment and Sustainability, Research Centre for Eco-Environmental Sciences, Chinese Academy of Sciences, Beijing 100085, China*

Bin Hu − *Key Lab of Aquatic Chemistry, State Key Lab of Regional Environment and Sustainability, Research Centre for Eco-Environmental Sciences, Chinese Academy of Sciences, Beijing 100085, China*

Walter van der Meer − *Membrane Science and Technology, Faculty of Science and Technology, University of Twente, Enschede 7500AE, The Netherlands*

Mark C. M. van Loosdrecht − *Department of Biotechnology, Delft University of Technology, Delft 2629 HZ, The Netherlands;* orcid.org/0000-0003-0658-4775

Martin Pabst − *Department of Biotechnology, Delft University of Technology, Delft 2629 HZ, The Netherlands*

Complete contact information is available at: https://pubs.acs.org/10.1021/acs.est.5c18277

Author Contributions

¶Y.Z. and X.W. contributed equally to this work. Y.Z. and X.W. conceived and designed experiments. Y.Z. and X.W. collected samples and associated metadata and performed experiments. Y.Z., X.D., G.L., X.W., B.H., and X.L. analyzed and visualized the data, Y.Z. and X.W. drafted the manuscript. W.v.d.M., M.v.L., G.L., and M.P. provided comprehensive supervision and support in methodology and data analysis from start to finish. All authors carried out writing, editing, and approved the final manuscript.

Notes

Code availability: All codes used in this study are publicly available.

The authors declare no competing financial interest.

■ ACKNOWLEDGMENTS

The present work has been financially supported by the National Natural Science Foundation of China (grant numbers: 52300190, 52525003, 42330705, 42473089). Yujia Zhai was supported by Beijing Normal University Tang Scholar.

■ REFERENCES

(1) Kuehn, W.; Mueller, U. Riverbank Filtration: An Overview. *J. - Am. Water Works Assoc.* **2000**, *92*, 60−69.

(2) Maeng, S. K.; Sharma, S. K.; Lekkerkerker-Teunissen, K.; Amy, G. L. Occurrence and fate of bulk organic matter and pharmaceutically active compounds in managed aquifer recharge: A review. *Water Res.* **2011**, *45*, 3015−3033.

(3) Sontheimer, H. Experience With Riverbank Filtration Along the Rhine River. *J. - Am. Water Works Assoc.* **1980**, *72*, 386−390.

(4) Barbosa, M. O.; Moreira, N. F. F.; Ribeiro, A. R.; Pereira, M. F. R.; Silva, A. M. T. Occurrence and removal of organic micropollutants: An overview of the watch list of EU Decision 2015/495. *Water Res.* **2016**, *94*, 257−279.

(5) Schwarzenbach, R. P.; Escher, B. I.; Fenner, K.; Hofstetter, T. B.; Johnson, C. A.; von Gunten, U.; Wehrli, B. The Challenge of Micropollutants in Aquatic Systems. *Science* **2006**, *313*, 1072−1077.

(6) Daughton, C. G.; Ternes, T. A. Pharmaceuticals and personal care products in the environment: agents of subtle change? *Environ. Health Perspect.* **1999**, *107*, 907−938.
(7) Wilkinson, J.; Hooda, P. S.; Barker, J.; Barton, S.; Swinden, J. Occurrence, fate and transformation of emerging contaminants in water: An overarching review of the field. *Environ. Pollut.* **2017**, *231*, 954−970.
(8) Wang, J.; de Ridder, D.; van der Wal, A.; Sutton, N. B. Harnessing biodegradation potential of rapid sand filtration for organic micropollutant removal from drinking water: A review. *Crit. Rev. Environ. Sci. Technol.* **2021**, *51*, 2086−2118.
(9) Ebrahimzadeh, S.; Wols, B.; Azzellino, A.; Kramer, F.; van der Hoek, J. P. Removal of organic micropollutants in a drinking water treatment plant by powdered activated carbon followed by rapid sand filtration. *Journal of Water Process Engineering* **2022**, *47*, 102792.
(10) Coha, M.; Farinelli, G.; Tiraferri, A.; Minella, M.; Vione, D. Advanced oxidation processes in the removal of organic substances from produced water: Potential, configurations, and research needs. *Chemical Engineering Journal* **2021**, *414*, 128668.
(11) Albergamo, V.; Blankert, B.; Cornelissen, E. R.; Hofs, B.; Knibbe, W.-J.; van der Meer, W.; de Voogt, P. Removal of polar organic micropollutants by pilot-scale reverse osmosis drinking water treatment. *Water Res.* **2019**, *148*, 535−545.
(12) Maeng, S. K.; Ameda, E.; Sharma, S. K.; Grützmacher, G.; Amy, G. L. Organic micropollutant removal from wastewater effluent-impacted drinking water sources during bank filtration and artificial recharge. *Water Res.* **2010**, *44*, 4003−4014.
(13) Zhao, J.; Fang, S.; Liu, G.; Qi, W.; Bai, Y.; Liu, H.; Qu, J. Role of ammonia-oxidizing microorganisms in the removal of organic micropollutants during simulated riverbank filtration. *Water Res.* **2022**, *226*, 119250.
(14) van Driezum, I. H.; Derx, J.; Oudega, T. J.; Zessner, M.; Naus, F. L.; Saracevic, E.; Kirschner, A. K. T.; Sommer, R.; Farnleitner, A. H.; Blaschke, A. P. Spatiotemporal resolved sampling for the interpretation of micropollutant removal during riverbank filtration. *Sci. Total Environ.* **2019**, *649*, 212−223.
(15) Bourg, A. C. M.; Bertin, C. Biogeochemical processes during the infiltration of river water into an alluvial aquifer. *Environ. Sci. Technol.* **1993**, *27*, 661−666.
(16) Ju, F.; Zhang, T. Bacterial assembly and temporal dynamics in activated sludge of a full-scale municipal wastewater treatment plant. *ISME J.* **2015**, *9*, 683−695.
(17) Lyu, B.; Manna, B.; Zhou, X.; Leung, I. K. H.; Singhal, N. Microbial metabolic enzymes, pathways and microbial hosts for co-metabolic degradation of organic micropollutants in wastewater. *Water Res.* **2025**, *276*, 123229.
(18) Bradley, P. M.; Journey, C. A.; Romanok, K. M.; Barber, L. B.; Buxton, H. T.; Foreman, W. T.; Furlong, E. T.; Glassmeyer, S. T.; Hladik, M. L.; Iwanowicz, L. R.; Jones, D. K.; Kolpin, D. W.; Kuivila, K. M.; Loftin, K. A.; Mills, M. A.; Meyer, M. T.; Orlando, J. L.; Reilly, T. J.; Smalling, K. L.; Villeneuve, D. L. Expanded Target-Chemical Analysis Reveals Extensive Mixed-Organic-Contaminant Exposure in U.S. Streams. *Environ. Sci. Technol.* **2017**, *51*, 4792−4802.
(19) Helbling, D. E.; Hollender, J.; Kohler, H.-P. E.; Singer, H.; Fenner, K. High-Throughput Identification of Microbial Transformation Products of Organic Micropollutants. *Environ. Sci. Technol.* **2010**, *44*, 6621−6627.
(20) Česen, M.; Heath, D.; Krivec, M.; Košmrlj, J.; Kosjek, T.; Heath, E. Seasonal and spatial variations in the occurrence, mass loadings and removal of compounds of emerging concern in the Slovene aqueous environment and environmental risk assessment. *Environ. Pollut.* **2018**, *242*, 143−154.
(21) Wingett, S. W.; Andrews, S. FastQ Screen: A tool for multi-genome mapping and quality control. *F1000Res.* **2018**, *7*, 1338.
(22) Ewels, P.; Magnusson, M.; Lundin, S.; Käller, M. MultiQC: summarize analysis results for multiple tools and samples in a single report. *Bioinformatics* **2016**, *32*, 3047−3048.
(23) Bolger, A. M.; Lohse, M.; Usadel, B. Trimmomatic: a flexible trimmer for Illumina sequence data. *Bioinformatics* **2014**, *30*, 2114−2120.
(24) Calderón-Franco, D.; Sarelse, R.; Christou, S.; Pronk, M.; van Loosdrecht, M. C. M.; Abeel, T.; Weissbrodt, D. G. Metagenomic profiling and transfer dynamics of antibiotic resistance determinants in a full-scale granular sludge wastewater treatment plant. *Water Res.* **2022**, *219*, 118571.
(25) Wood, D. E.; Lu, J.; Langmead, B. Improved metagenomic analysis with Kraken 2. *Genome Biol.* **2019**, *20*, 257.
(26) Breitwieser, F. P.; Salzberg, S. L. Pavian: interactive analysis of metagenomics data for microbiome studies and pathogen identification. *Bioinformatics* **2020**, *36*, 1303−1304.
(27) McMurdie, P. J.; Holmes, S. phyloseq: An R Package for Reproducible Interactive Analysis and Graphics of Microbiome Census Data. *PLoS One* **2013**, *8*, No. e61217.
(28) Nurk, S.; Meleshko, D.; Korobeynikov, A.; Pevzner, P. A. metaSPAdes: a new versatile metagenomic assembler. *Genome Res.* **2017**, *27*, 824−834.
(29) Hyatt, D.; Chen, G.-L.; LoCascio, P. F.; Land, M. L.; Larimer, F. W.; Hauser, L. J. Prodigal: prokaryotic gene recognition and translation initiation site identification. *BMC Bioinf.* **2010**, *11*, 119.
(30) Steinegger, M.; Söding, J. MMseqs2 enables sensitive protein sequence searching for the analysis of massive data sets. *Nat. Biotechnol.* **2017**, *35*, 1026−1028.
(31) Cantalapiedra, C. P.; Hernández-Plaza, A.; Letunic, I.; Bork, P.; Huerta-Cepas, J. eggNOG-mapper v2: Functional Annotation, Orthology Assignments, and Domain Prediction at the Metagenomic Scale. *Mol. Biol. Evol.* **2021**, *38*, 5825−5829.
(32) Aroney, S. T.; Newell, R. J.; Nissen, J.; Camargo, A. P.; Tyson, G. W.; Woodcroft, B. J. *Coverm: Read Coverage Calculator for Metagenomics*; Zenodo, 2024; p 10531254.
(33) Sivakumar, S.; Anitha, P.; Ramesh, B.; Suresh, G. Analysis of EAWAG-BBD pathway prediction system for the identification of malathion degrading microbes. *Bioinformation* **2017**, *13*, 73−77.
(34) Wicker, J.; Lorsbach, T.; Gütlein, M.; Schmid, E.; Latino, D.; Kramer, S.; Fenner, K. enviPath − The environmental contaminant biotransformation pathway resource. *Nucleic Acids Res.* **2016**, *44*, D502−D508.
(35) Wickham, H. ggplot2. *WIREs Computational Statistics* **2011**, *3*, 180−185.
(36) Lyu, F.; Han, F.; Ge, C.; Mao, W.; Chen, L.; Hu, H.; Chen, G.; Lang, Q.; Fang, C. OmicStudio: A composable bioinformatics cloud platform with real-time feedback that can generate high-quality graphs for publication. *iMeta* **2023**, *2*, No. e85.
(37) Munz, M.; Oswald, S. E.; Schäfferling, R.; Lensing, H.-J. Temperature-dependent redox zonation, nitrate removal and attenuation of organic micropollutants during bank filtration. *Water Res.* **2019**, *162*, 225−235.
(38) Miettinen, I. T.; Vartiainen, T.; Martikainen, P. J. Bacterial enzyme activities in ground water during bank filtration of lake water. *Water Res.* **1996**, *30*, 2495−2501.
(39) Inniss, E. C. *Water Encyclopedia*, 2005; pp 399−400.
(40) Cronk, J. K.; Fennessy, M. S. *Wetland Plants: Biology and Ecology*; CRC Press, 2016.
(41) Barba, C.; Folch, A.; Gaju, N.; Sanchez-Vila, X.; Carrasquilla, M.; Grau-Martínez, A.; Martínez-Alonso, M. Microbial community changes induced by Managed Aquifer Recharge activities: linking hydrogeological and biological processes. *Hydrol. Earth Syst. Sci.* **2019**, *23*, 139−154.
(42) Kim, H.; Mok, J.-K.; Park, Y.; Kaown, D.; Lee, K.-K. Composition of Groundwater Bacterial Communities before and after Air Surging in a Groundwater Heat Pump System According to a Pyrosequencing Assay. *Water* **2017**, *9*, 891.
(43) Mosley, O. E.; Gios, E.; Handley, K. M. Implications for nitrogen and sulphur cycles: phylogeny and niche-range of Nitrospirota in terrestrial aquifers. *ISME Communications* **2024**, *4*, ycae047.
(44) Cui, G.; Su, X.; Zheng, S.; Tong, S.; Jiang, M. Hydrological and biogeochemical processes controlling riparian groundwater quantity

https://doi.org/10.1021/acs.est.5c18277
Environ. Sci. Technol. 2026, 60, 5804−5816

and quality during riverbank filtration. *Environ. Pollut.* **2024**, *350*, 124020.
(45) Ginige, M. P.; Kaksonen, A. H.; Morris, C.; Shackelton, M.; Patterson, B. M. Bacterial community and groundwater quality changes in an anaerobic aquifer during groundwater recharge with aerobic recycled water. *FEMS Microbiol. Ecol.* **2013**, *85*, 553−567.
(46) Ino, K.; Konno, U.; Kouduka, M.; Hirota, A.; Togo, Y. S.; Fukuda, A.; Komatsu, D.; Tsunogai, U.; Tanabe, A. S.; Yamamoto, S.; Iwatsuki, T.; Mizuno, T.; Ito, K.; Suzuki, Y. Deep microbial life in high-quality granitic groundwater from geochemically and geographically distinct underground boreholes. *Environ. Microbiol. Rep.* **2016**, *8*, 285−294.
(47) Ju, Y.; Park, K.-W.; Kwon, E.; Kaown, D.; Jun, S. C.; Park, J.; Lee, K.-K. Evaluating radionuclide mobility in groundwater recharge areas of fractured natural barrier systems using multiple isotopes and microbial indicators. *J. Hazard. Mater.* **2025**, *482*, 136571.
(48) Guengerich, F. P. Intersection of the Roles of Cytochrome P450 Enzymes with Xenobiotic and Endogenous Substrates: Relevance to Toxicity and Drug Interactions. *Chem. Res. Toxicol.* **2017**, *30*, 2−12.
(49) Wang, S.; Zhu, G.; Zhuang, L.; Li, Y.; Liu, L.; Lavik, G.; Berg, M.; Liu, S.; Long, X.-E.; Guo, J.; Jetten, M. S. M.; Kuypers, M. M. M.; Li, F.; Schwark, L.; Yin, C. Anaerobic ammonium oxidation is a major N-sink in aquifer systems around the world. *ISME J.* **2020**, *14*, 151−163.
(50) Regnery, J.; Gerba, C. P.; Dickenson, E. R. V.; Drewes, J. E. The importance of key attenuation factors for microbial and chemical contaminants during managed aquifer recharge: A review. *Crit. Rev. Environ. Sci. Technol.* **2017**, *47*, 1409−1452.
(51) Hiscock, K. M.; Grischek, T. Attenuation of groundwater pollution by bank filtration. *Journal of Hydrology* **2002**, *266*, 139−144.
(52) Huntscha, S.; Rodriguez Velosa, D. M.; Schroth, M. H.; Hollender, J. Degradation of Polar Organic Micropollutants during Riverbank Filtration: Complementary Results from Spatiotemporal Sampling and Push−Pull Tests. *Environ. Sci. Technol.* **2013**, *47*, 11512−11521.
(53) Hollender, J.; Rothardt, J.; Radny, D.; Loos, M.; Epting, J.; Huggenberger, P.; Borer, P.; Singer, H. Comprehensive micropollutant screening using LC-HRMS/MS at three riverbank filtration sites to assess natural attenuation and potential implications for human health. *Water Res.:X* **2018**, *1*, 100007.
(54) Bertelkamp, C.; Reungoat, J.; Cornelissen, E. R.; Singhal, N.; Reynisson, J.; Cabo, A. J.; van der Hoek, J. P.; Verliefde, A. R. D. Sorption and biodegradation of organic micropollutants during river bank filtration: A laboratory column study. *Water Res.* **2014**, *52*, 231−241.
(55) Zearley, T. L.; Summers, R. S. Removal of Trace Organic Micropollutants by Drinking Water Biological Filters. *Environ. Sci. Technol.* **2012**, *46*, 9412−9419.
(56) Stiegler, A. N.; Cecchetti, A. R.; Scholes, R. C.; Sedlak, D. L. Persistent Trace Organic Contaminants Are Transformed Rapidly under Sulfate- and Fe(III)-Reducing Conditions in a Nature-Based Subsurface Water Treatment System. *Environ. Sci. Technol.* **2023**, *57*, 16616−16627.
(57) Abdelrady, A.; Sharma, S.; Sefelnasr, A.; Abogbal, A.; Kennedy, M. Investigating the impact of temperature and organic matter on the removal of selected organic micropollutants during bank filtration: A batch study. *J. Environ. Chem. Eng.* **2019**, *7*, 102904.
(58) Sanz-Prat, A.; Greskowiak, J.; Burke, V.; Rivera Villarreyes, C. A.; Krause, J.; Monninkhoff, B.; Sperlich, A.; Schimmelpfennig, S.; Duennbier, U.; Massmann, G. A model-based analysis of the reactive transport behaviour of 37 trace organic compounds during field-scale bank filtration. *Water Res.* **2020**, *173*, 115523.
(59) Erdélyi, N.; Gere, D.; Fekete, E.; Nyiri, G.; Engloner, A.; Tóth, A.; Madarász, T.; Szűcs, P.; Nagy-Kovács, Z. A.; Pándics, T.; Vargha, M. Transport model-based method for estimating micropollutant removal efficiency in riverbank filtration. *Water Res.* **2025**, *275*, 123194.
(60) Albergamo, V.; Schollée, J. E.; Schymanski, E. L.; Helmus, R.; Timmer, H.; Hollender, J.; de Voogt, P. Nontarget Screening Reveals Time Trends of Polar Micropollutants in a Riverbank Filtration System. *Environ. Sci. Technol.* **2019**, *53*, 7584−7594.
(61) Diem, S.; Cirpka, O. A.; Schirmer, M. Modeling the dynamics of oxygen consumption upon riverbank filtration by a stochastic−convective approach. *Journal of Hydrology* **2013**, *505*, 352−363.
(62) Rudolf von Rohr, M.; Hering, J. G.; Kohler, H.-P. E.; von Gunten, U. Column studies to assess the effects of climate variables on redox processes during riverbank filtration. *Water Res.* **2014**, *61*, 263−275.
(63) Schaper, J. L.; Seher, W.; Nützmann, G.; Putschew, A.; Jekel, M.; Lewandowski, J. The fate of polar trace organic compounds in the hyporheic zone. *Water Res.* **2018**, *140*, 158−166.
(64) Schaper, J. L.; Posselt, M.; Bouchez, C.; Jaeger, A.; Nuetzmann, G.; Putschew, A.; Singer, G.; Lewandowski, J. Fate of Trace Organic Compounds in the Hyporheic Zone: Influence of Retardation, the Benthic Biolayer, and Organic Carbon. *Environ. Sci. Technol.* **2019**, *53*, 4224−4234.
(65) Höhne, A.; Müller, B. M.; Schulz, H.; Dara, R.; Posselt, M.; Lewandowski, J.; McCallum, J. L. Fate of trace organic compounds in the hyporheic zone: Influence of microbial metabolism. *Water Res.* **2022**, *224*, 119056.
(66) Reith, C. J.; Spahr, S.; Putschew, A.; Lewandowski, J. Attenuation of trace organic compounds along hyporheic flow paths in a lowland sandbed stream. *Journal of Hydrology* **2023**, *624*, 129905.
(67) Reemtsma, T.; Miehe, U.; Duennbier, U.; Jekel, M. Polar pollutants in municipal wastewater and the water cycle: Occurrence and removal of benzotriazoles. *Water Res.* **2010**, *44*, 596−604.
(68) Trček, B.; Žigon, D.; Zidar, V. K.; Auersperger, P. The fate of benzotriazole pollutants in an urban oxic intergranular aquifer. *Water Res.* **2018**, *131*, 264−273.
(69) Nikolenko, O.; Labad, F.; Pujades, E.; Scheiber, L.; Pérez, S.; Ginebreda, A.; Jurado, A. Combination of multivariate data analysis and mixing modelling to assess tracer potential of contaminants of emerging concern in aquifers. *Environ. Pollut.* **2024**, *341*, 123020.
(70) Liu, Y.-S.; Ying, G.-G.; Shareef, A.; Kookana, R. S. Biodegradation of three selected benzotriazoles in aquifer materials under aerobic and anaerobic conditions. *J. Contam. Hydrol.* **2013**, *151*, 131−139.
(71) Deng, Z.; Hu, B.; He, C.; Zhang, L.; Zhao, X.; Zhang, X. Benzotriazole aerobic biodegradation by activated sludge and Bacillus sp. DH-12: Performance, community succession, and transformation products characterization. *J. Environ. Chem. Eng.* **2024**, *12*, 113671.
(72) Wang, J.; Poursat, B. A. J.; Feng, J.; de Ridder, D.; Zhang, C.; van der Wal, A.; Sutton, N. B. Exploring organic micropollutant biodegradation under dynamic substrate loading in rapid sand filters. *Water Res.* **2022**, *221*, 118832.
(73) Trejo-Castillo, R.; El Kassis, E. G.; Cuervo-López, F.; Texier, A.-C. Cometabolic biotransformation of benzotriazole in nitrifying batch cultures. *Chemosphere* **2021**, *270*, 129461.
(74) Henning, N.; Kunkel, U.; Wick, A.; Ternes, T. A. Biotransformation of gabapentin in surface water matrices under different redox conditions and the occurrence of one major TP in the aquatic environment. *Water Res.* **2018**, *137*, 290−300.
(75) Sun, H.; Xia, J.; Wu, B.; Ren, H.; Zhang, X.; Ye, L. Aerobic starvation treatment of activated sludge enhances the degradation efficiency of refractory organic compounds. *Water Res.* **2022**, *224*, 119069.
(76) Cao, L.; Garcia, S. L.; Wurzbacher, C. Profiling trace organic chemical biotransformation genes, enzymes and associated bacteria in microbial model communities. *J. Hazard. Mater.* **2025**, *485*, 136811.

https://doi.org/10.1021/acs.est.5c18277
Environ. Sci. Technol. 2026, 60, 5804−5816